This is the accepted manuscript version of the contribution published as:

Ebert, A., **Goss, K.-U.** (2020):
Predicting uncoupling toxicity of organic acids based on their molecular structure using a biophysical model
Chem. Res. Toxicol. **33** (7), 1835 – 1844

The publisher's version is available at:

http://dx.doi.org/10.1021/acs.chemrestox.0c00063

Chemical Research in Toxicology®

Subscriber access provided by HELMHOLTZ ZENTRUM UMWELTFORSCHUNG

Article

Predicting uncoupling toxicity of organic acids based on their molecular structure using a biophysical model

Andrea Ebert, and Kai-Uwe Goss

Chem. Res. Toxicol., **Just Accepted Manuscript** • DOI: 10.1021/acs.chemrestox.0c00063 • Publication Date (Web): 28 May 2020

Downloaded from pubs.acs.org on June 12, 2020

Just Accepted

"Just Accepted" manuscripts have been peer-reviewed and accepted for publication. They are posted online prior to technical editing, formatting for publication and author proofing. The American Chemical Society provides "Just Accepted" as a service to the research community to expedite the dissemination of scientific material as soon as possible after acceptance. "Just Accepted" manuscripts appear in full in PDF format accompanied by an HTML abstract. "Just Accepted" manuscripts have been fully peer reviewed, but should not be considered the official version of record. They are citable by the Digital Object Identifier (DOI®). "Just Accepted" is an optional service offered to authors. Therefore, the "Just Accepted" Web site may not include all articles that will be published in the journal. After a manuscript is technically edited and formatted, it will be removed from the "Just Accepted" Web site and published as an ASAP article. Note that technical editing may introduce minor changes to the manuscript text and/or graphics which could affect content, and all legal disclaimers and ethical guidelines that apply to the journal pertain. ACS cannot be held responsible for errors or consequences arising from the use of information contained in these "Just Accepted" manuscripts.

is published by the American Chemical Society. 1155 Sixteenth Street N.W., Washington, DC 20036

Published by American Chemical Society. Copyright © American Chemical Society. However, no copyright claim is made to original U.S. Government works, or works produced by employees of any Commonwealth realm Crown government in the course of their duties.

1

Predicting uncoupling toxicity of organic acids based on their molecular structure using a biophysical model

Andrea Ebert*[,†,‡], Kai Uwe Goss[†,§]

[†] Analytical Environmental Chemistry, Helmholtz Centre for Environmental Research – UFZ, Leipzig, Germany
[‡] Institute of Biophysics, Johannes Kepler University, Linz, Austria
[§] Institute of Chemistry, Martin Luther University, Halle, Germany

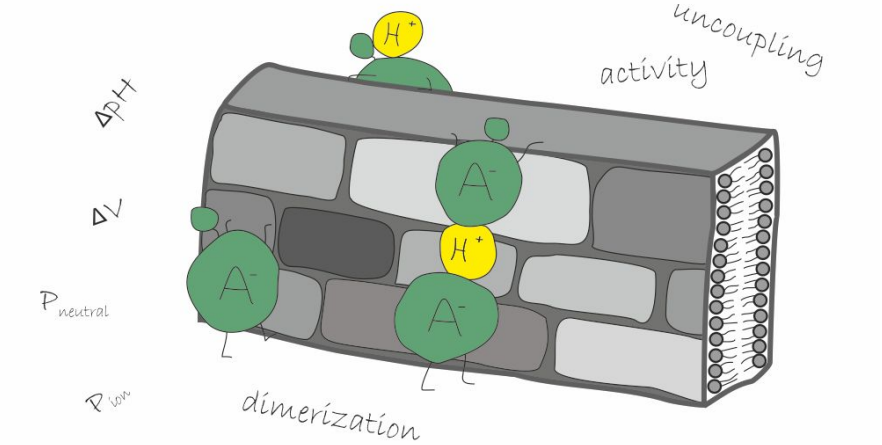

keywords: uncoupling of phosphorylation; protonophore; pH-dependent toxicity; mechanistic prediction model, dimerization; ion-trapping

Abstract:

We present a purely mechanistic model to predict protonophoric uncoupling activity EC_w of organic acids. All required input information can be derived from their chemical structure. This makes it a convenient predictive model to gain valuable information on the toxicity of organic chemicals already at an early stage of development of new commercial chemicals (e.g. in agriculture or pharmaceutical industries). A critical component of the model is the consideration of the possible formation of heterodimers from the neutral and anionic monomer, and its permeation through the membrane. The model was tested against literature data measured in chromatophores, submitochondrial particles, isolated mitochondria, and intact green algae cells with good success. It was also possible to reproduce pH-dependencies in isolated mitochondria and intact cells. Besides the prediction of the EC_w, the

mechanistic nature of the model allows to draw direct conclusions on the impact of single input factors, such as pH- and voltage- gradients across the membrane, the anionic and neutral membrane permeability, and the heterodimerization constant. These insights are of importance in drug design or chemical regulation.

Introduction:

According to Mitchell's chemiosmotic theory [1], the transmembrane electrochemical proton gradient across the inner mitochondrial membrane is essential for the synthesis of ATP. A protonophoric uncoupler decreases/dissipates this proton gradient by shuttling protons across the inner membrane of the mitochondria, generating heat instead of ATP. The uncoupling process is driven by the chemiosmotic gradient itself, and may therefore continue, as long as the gradient exists. Consequently, the respiratory chain and ATP synthesis are uncoupled [2], while neither the activities of the respiratory chain nor the ATP synthase are inhibited [3]. To a certain extent such uncoupling happens naturally by uncoupling proteins, which is important for the regulation of the mitochondrial membrane potential [4]. However, any extensive bypass of the ATP synthase through the exposure to chemical uncouplers can deprive the cell of energy and thus lead to a toxic effect. While a low uncoupler concentration may still be compensated for by an increased respiration rate, higher concentrations will lead to a collapse of the membrane potential and thus inhibit ATP synthesis.

Already in the early seventies of the last century, a reasonably good correlation between critical uncoupling effects (concentration at which state 4 respiration in rat liver mitochondria was doubled) and a specific increase of electrical conductance in black lipid membranes BLM was observed [5]. Many quantitative structure-activity relationship (QSAR) models (e.g. [6–11]) have been developed to predict uncoupling toxicity, often based on the octanol/water partition coefficient and the pK_a as descriptors. More recently, a mechanistically based approach to predict uncoupling activity also identified the permeability of the ionic species across the membrane as the most important descriptor in a QSAR model [12]. However, as this model does not consider other possible limiting effects, like the membrane

permeability of the neutral chemical species, it tends to overestimate the uncoupling activity for compounds with low pK_a (<3). For that reason, the applicable pK_a range was defined from 3-9 [12]. Its ability to predict uncoupling activity is limited to pH7, because pH- and electrical gradients across the membrane are not explicitly considered in the model, but covered by calibrated coefficients.

Already in 1980, McLaughlin and Dilger [13] developed a biophysical model with physiological input data (membrane permeability of anionic and neutral species, pK_a, transmembrane potential and pH) and solved it numerically to predict the flux of protons through the membrane of mitochondria and submitochondrial particles for 2,4,6-trinitrophenol. This way, they were able to solve the discrepancy as to why 2,4,6-trinitrophenol would uncouple submitochondrial particles (their pH- and electrical potential gradient is reversed in comparison to mitochondria), but not mitochondria. Their calculations showed that the effect of the uncoupler was limited by the permeability of its neutral species, and thus stronger for submitochondrial particles due to the larger neutral fraction inside the particles, where the pH is lowered.

Due to the lack of experimental or predicted anionic membrane permeability data though, neither the direct correlation between uncoupling and electrical conductance, nor the more elaborate mechanistic physiological model of McLaughlin and Dilger found a widespread application.

Recent advances in the prediction of anionic permeation through lipid bilayers [14,15] should now allow the application of a purely mechanistic biophysical prediction model for pH-dependent uncoupling toxicity.

Two important effects are not yet implemented in the biophysical model of McLaughlin and Dilger: First, a potential ion-trapping effect [16] that can occur in any organism with a quasi neutral internal pH that is living in an acidic or alkaline aqueous environment, and second, the formation and subsequent permeation of anionic heterodimers as an additional proton carrier through the membrane. Both effects can lead to an underestimation of uncoupling toxicity when missing in the calculations:The former effect, ion-trapping, can lead to an up- or down-concentration of the uncoupler inside a cell or an organism, and thus to a strong pH-dependence of the uncoupling effect. Yet, for uncoupling activity,

pH-dependent measurements are rare, and in some cases, at first glance, do not seem to be explainable by Mitchell's chemiosmotic theory [17]. The latter effect, the permeation of the heterodimer across the membrane, can significantly enhance the uncoupling effect [18]. Together with their anion A^- some acids AH form a heterodimer AHA^- [19], whose membrane permeability is typically greater than the permeability of the pure anion.

This implies the need for a more complex biophysical model of uncoupling, but also the additional need to predict dimerization constants in water. This is done here in accordance with the method described in Ref. [20,21] for the computation of reactions in solution.

The goal of the presented work therefore was to extend the biophysical model of McLaughlin and Dilger from isolated mitochondria to intact cells including effects such as ion-trapping and heterodimer formation and permeation. Furthermore, we adopted methods that allow the prediction of all needed input parameters to the model based on the molecular structure of the chemical. Hence, all input parameters, such as anionic permeability or the dimerization constant of the heterodimer in water, can now be calculated based on quantum chemical and COSMO-RS (Conductor-like Screening Model for Realistic Solvation) [22] calculations. Finally, we tested the model on literature uncoupling data in different biological systems, and analyzed the impact of various input parameters.

Methods:

Monomeric permeation model

Organisms exposed to constant concentrations of a chemical will rather quickly (within hours) arrive at steady state conditions concerning the internal concentration of this chemical. Therefore, toxicity testing is usually performed for such conditions and a mechanistic model for uncoupling activity should also be based on a steady state situation. This means that a model of protonophoric uncoupling (see Figure 1) describes a situation where the net flux $\Phi_{AH_{2,1}}$ of the associated form AH of

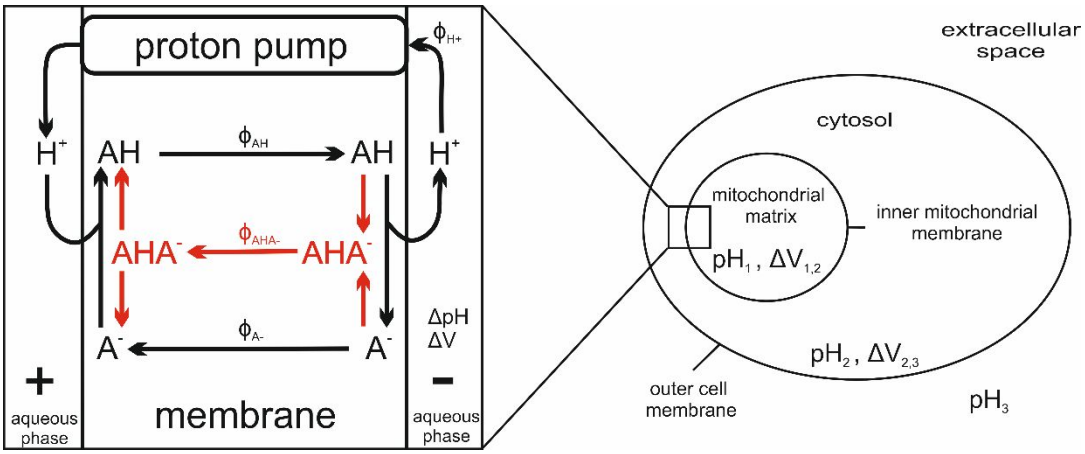

Figure 1 Model of uncoupling. (Left) Zoom-in on the inner mitochondrial membrane: Driven by a chemical potential and electrical potential ΔV, the dissociated species of a weak acid A^- traverses the membrane. On the other side of the membrane, A^- picks up a proton (according to pH), regains its neutral form AH and – following a concentration gradient – diffuses back. By this cycle, protons are shuttled across the membrane, dissipating the proton gradient created by the proton pumps of the respiratory chain. The proton pumps thus have to increase their pumping rate to sustain the proton gradient. Anionic permeation may also be dominated by the permeation of the heterodimer AHA^- (see red permeation pathway, heterodimer flux Φ_{AHA^-}), whose membrane permeability is typically greater than the permeability of the pure anion. (Right) Schematic model of a eukaryotic cell (very simplified and not up to scale): (1) mitochondrial matrix, (2) cytosol, (3) extracellular space.

the weak acid from the cytosol to the mitochondrial matrix has to equal the opposing net flux $\Phi_{A^-_{1,2}}$ of the charged dissociated form A^- from the mitochondrial matrix to the cytosol:

$$\Phi_{AH_{2,1}} = \Phi_{A^-_{1,2}} \quad (1)$$

Neutral fluxes result from chemical gradients, while ionic fluxes result from both chemical and electrical gradients, see Eq. S1-1 and S1-2 respectively for the mathematical expressions.

For a model that predicts uncoupling activity , we now have to combine this biophysical approach with a quantitative information on the extent of proton shuttling. In the steady state situation, the flux of shuttled H^+ is balanced by a flux of H^+ of the same magnitude in opposing direction created by an increased activity of the proton pumps:

6

$$\Delta\Phi_{H^+{}_{1,2}} = \Phi_{AH_{2,1}} \quad (2)$$

where $\Delta\Phi_{H^+{}_{1,2}}$ is the additional proton flux pumped from the mitochondrial matrix to the cytosol as a response to the uncoupler and $\Phi_{AH_{2,1}}$ is the opposing flux of the associated form AH of the weak acid from the cytosol to the mitochondrial matrix.

Uncoupling activity is measured as effective freely dissolved concentration, which signifies the concentration of the uncoupler that produces a specific biological response. For uncoupling activity, the doubling of the respiration rate in state 4 respiration is regarded as a typical toxic endpoint [8]. Combining Eq. 1 and 2, the respective freely dissolved uncoupler concentration in the cytosol [A_2] can be expressed as:

$$[A_2] = \Delta\Phi_{H^+{}_{1,2}} * \frac{\frac{1}{f_{A^-,1} * P_{A^-{}_i}} * \frac{1 - \exp\left(-\frac{zF}{RT}\Delta V_{1,2}\right)}{\frac{zF}{RT}\Delta V_{1,2}} + \frac{1}{f_{AH,1} * P_{AH}}}{\frac{f_{AH,2}}{f_{AH,1}} - \frac{f_{A^-,2}}{f_{A^-,1}} * \exp\left(-\frac{zF}{RT}\Delta V_{1,2}\right)} \quad (3)$$

where P_{AH} and $P_{A^-_i}$ are the permeabilities of AH and A^- across the inner membrane, [A_1] and [A_2] are the freely dissolved concentrations, $f_{AH,1}$ and $f_{AH,2}$ the neutral fractions and $f_{A^-,1}$ and $f_{A^-,2}$ the anionic fractions of the weak acid in the mitochondrial matrix and the cytosol respectively. $\Delta V_{1,2}$ is the electrical potential difference between the mitochondrial matrix and the cytosol (negative if the mitochondrial matrix is negatively charged), z the valence of the ion (-1 for anions), F the Faraday constant, R the gas constant, and T the temperature.

In case of isolated mitochondria, [A_2] corresponds to the effective concentration EC_w. If we consider intact cells, the net flux of A has to be zero in the steady state at the outer membrane as well:

7

$$\Phi_{AH_{3,2}} = \Phi_{A^-{}_{2,3}} \quad (4)$$

where $\Phi_{AH_{3,2}}$ is the net flux of the associated form AH of the weak acid from the extracellular space to the cytosol, and $\Phi_{A^-_{2,3}}$ is the opposing net flux of the dissociated form A^- from the cytosol to the extracellular space.

Inserting the expressions for the neutral and ionic flux in Eq. 4, we get an expression for the freely dissolved uncoupler concentration in the extracellular space [A_3], which is the critical, freely dissolved exposure concentration EC_w at which uncoupling activity would be expected:

$$[A_3] = [A_2] * \frac{P_{A^-{}_o} * f_{A^-,2} * \dfrac{\frac{zF}{RT}\Delta V_{2,3}}{1 - \exp\left(-\frac{zF}{RT}\Delta V_{2,3}\right)} + f_{AH,2} * P_{AH}}{P_{AH} * f_{AH,3} + P_{A^-{}_o} * f_{A^-,3} \dfrac{\exp\left(-\frac{zF}{RT}\Delta V_{2,3}\right) * \frac{zF}{RT}\Delta V_{2,3}}{1 - \exp\left(-\frac{zF}{RT}\Delta V_{2,3}\right)}} \quad (5)$$

where $P_{A^-_o}$ is the permeability of A^- across the outer membrane of the cell. Anionic permeabilities across the inner mitochondrial membrane and across the outer membrane must be kept apart, because the ionic permeability through the inner mitochondrial membrane is reported to be orders of magnitude higher than those through artificial membranes, which we assume to have similar permeabilities as the outer cell membrane. This effect is supposedly caused by an increase of the dielectric constant inside the mitochondrial membrane due to the high amount of proteins [23,24].

Heterodimeric permeation model

The model discussed above can be extended to include heterodimer AHA^- permeation (see red permeation pathway in Figure 1). When AHA^- permeation is considered, again there is no net flux of A across the membrane, and Eq. 1 is extended to:

8

$$\Phi_{AH_{2,1}} = \Phi_{A^-{}_{1,2}} + 2\Phi_{AHA^-{}_{1,2}} \quad (6)$$

Note: the factor 2 before the heterodimeric flux $\Phi_{AHA^-_{1,2}}$ from the mitochondrial matrix to the cytosol simply arises from the fact that 2 mol of compound A permeate the membrane for each mol of AHA^-.

Analogously, to maintain a net proton flux of zero (steady state conditions) across the membrane in case of heterodimer permeation, Eq. 2 needs to be expanded to:

$$\Delta\Phi_{H^+{}_{1,2}} = \Phi_{AH_{2,1}} - \Phi_{AHA^-{}_{1,2}} \quad (7)$$

In the case of intact cells, Eq. 4 has to be extended for heterodimer permeation considering that there is no net flux of A at the outer membrane in the steady state:

$$\Phi_{AH_{3,2}} = \Phi_{A^-{}_{2,3}} + 2\Phi_{AHA^-{}_{2,3}} \quad (8)$$

This system of equations including heterodimeric permeation can only be solved numerically. We implemented the equations in an Igor Pro (WaveMetrics, Lake Oswego, OR) script that can be found in the Supporting Information SI-3. See Sections S1-2 and S1-3 for a detailed derivation of the model.

Input parameters

Important input factors of our model can be categorized into compound specific and system specific parameters. Compound specific paramters, namely pK_a, dimerization constant $K_{D,W}$, neutral and anionic permeability are reported in a common database for all 164 investigated compounds in Table S2-1. In contrast, pH- and electrical potential gradients across the membrane and the increase in proton pumping rate ($\Delta\Phi_{H^+_{1,2}}$) at critical effect concentrations depend on the system and experimental setting at which the uncoupling activity was measured.

The following paragraphs deal with the individual parameters and their origin or calculation.

Compound specific parameters

Experimental input data were always preferred, but if none were available, predictive methods were used to generate the compound specific parameters. We used the software COSMOtherm [22,25] to predict membrane permeability *P* for both the neutral and the anionic species. COSMOtherm is an ab initio approach based on the COSMO-RS (Conductor-like Screening Model for Realistic Solvation) theory. Quantum chemical calculations (Turbomole [26]) are used to generate the surface charge densities of energetically optimized structures, so called COSMOfiles. Using COSMOconf [27], several conformers of the compounds can be created, which account for the fact that different conformers may be energetically more favorable in different solvents. Interactions (e.g. electrostatic, hydrogen bonding and van der Waals interactions) with other molecules are quantified as local interactions of these charge density surfaces, and pairwise interactions are averaged thermodynamically. Electronic group effects such as mesomeric or inductive effects are automatically considered, as are intramolecular interactions such as hydrogen bonding. See Ref. [22] for details. While the quantum chemical calculations may take hours to days on a standard computer, depending on compound size and flexibility, the COSMOtherm calculations based on the COSMOfiles will only take minutes.

According to the solubility diffusion model, the permeability depends on the partitioning into and the diffusion through the membrane [28]. Assuming that the nonpolar, aliphatic membrane core constitutes the main resistance for the permeation, hexadecane can be used as a surrogate to represent the inner part of the membrane. The calculation of the permeability can then be based on the partitioning from water into hexadecane. This may be done by simple correlations [14,29] or mechanistic models [30]. Here, hexadecane was used as a surrogate for the membrane core to predict anionic permeability of the outer cell membrane, while chlorodecane was used to predict anionic permeability of the mitochondrial membrane, because chlorodecane containing bilayers were shown to have

permeabilities similar to those of the inner mitochondrial membrane [24]. Chlorodecane has a larger dielectric constant than hexadecane and thus simulates the increased dielectric constant inside the mitochondrial membrane better than hexadecane. We assume no difference in permeability between artificial membranes and the inner mitochondrial membrane for neutral compounds. Neutral permeabilities through artificial membranes containing decane or chlorodecane as a solvent were shown to be similar within a factor of 2, and did not differ by more than a factor of 3 from mitochondrial membranes [31], because the change of dielectric constant inside the membrane does not seriously affect neutral compounds. It is unclear how well the permeabilities across artificial planar bilayers represent the membrane permeability of the outer cell membrane. Nevertheless, for simplification we will assume the permeability in the outer cell membrane as equal to the one in artificial systems. Different characteristics such as membrane lipid composition (cholesterol, sphingomyelin content,…), protein content, membrane asymmetry or the formation of lipid rafts could influence membrane permeability. But this uncertainty will only affect the calculations of the ion-trapping effect across the outer cell membrane for intact cells, not the calculations in the mitochondria themselves.

If not available in literature, pK_a values were predicted by the software COSMOtherm, because it performed better than JChem for Office (Excel) [32] in a validation with literature data, see Figure S1-2. The fractionation into neutral and anionic species was calculated using the Henderson-Hasselbalch equation.

The dimerization constant $K_{D,W}$ in water (unit: 1/M) is predicted using the software Turbomole and COSMOtherm, in accordance with a COSMO-RS approach for reactions in solution published in Ref. [20,21]. To this end, gas phase energies at zero Kelvin, being the Single Point Energies E_{SPE} (electronic energy) and the Zero Point Energy E_{ZPE} (vibrational correction), and the chemical potential at finite temperatures ΔG_{THERM} (due to rotational, translational, and vibrational degrees of freedom) are calculated in vacuum for all species using Turbomole. Vacuum was chosen as a reference system, to avoid disturbing effects due to the interaction with the solvent, e.g. water. Because we are finally

interested in the dimerization constant in water, transition from the gas phase to solution is described by the free energy of solvation ΔG_{SOLV} calculated with COSMOtherm. The dimerization constant is then calculated from the energy difference between the heterodimer and the combined energy of the two monomers. See Figure S1-1 for a detailed workflow on how to calculate the heterodimerization constant.

The uncoupler circles inside the membrane, shuttling protons across it without the need to actually leave the membrane. Thus, it may seem counter-intuitive to use the aqueous compound concentrations in the calculations. Yet, this is a consequence of water being our reference system, also in regard of membrane permeability. Choosing any other membrane layer as reference, considering the respective (different) compound concentrations in that layer and the respective (different) height of energy barriers for permeation, would lead to identical results.

System specific parameters

Information on externally applied pH must be taken from the respective literature. Typical pH- and potential- differences across the membrane of the tested biological systems have been extracted from literature, and are listed in Table S1-1. While Figure 1 depicts a typical constellation of gradients for mitochondria (negative electrical potential inside), pH- and potential- gradients are reversed in other scenarios, like submitochondrial particles or chromatophores (positive inside).

The second system specific input parameter is the proton flux across the mitochondrial membrane $\Delta\Phi_{H^+}$ due to uncoupling activity that would lead to the effect described by the toxic endpoint specified in the experiment. We estimated the critical proton flux $\Delta\Phi_{H^+}$ across the inner mitochondrial membrane due to the effective concentration of an uncoupler to be about $3*10^{-11}$ mol/(cm^2*s). Basis of the estimation was the empirical correlation found by Skulachev [5] between the concentration of a compound needed to double the State 4 respiration rate and the concentration needed to induce an increase in electrical conductivity in BLM. For confirmation, we also estimated the proton flux based

on measured respiration rates and found reasonable agreement between both estimates (see Sections S1-7 and S1-8 in the Supporting Information for details).

The $\Delta\Phi_{H^+}$ of $3*10^{-11}$ mol/(cm^2*s) was not only used for the toxic endpoint of the doubling of the respiration rate, but also for various other toxic endpoints such as reproduction inhibition and growth inhibition, because all these toxic endpoints are established indicators of uncoupling activity. A direct calibration for each specific endpoint might increase the accuracy of the prediction, because some endpoints might be more or less sensitive for uncoupling activity, but this was not done for reasons of simplicity and generality. The rate was only adapted in case of isolated mitochondria, to account for toxic endpoints of 50% or 100% (maximum) stimulation of the respiration rate instead of the doubling. Typical values of liver mitochondria oxidizing succinate in state 4 are about 15nmol O/min/$mg_{protein}$ and amount to about 100 nmol O/min/$mg_{protein}$ at maximum respiration[33]. The doubling would therefore correspond to an increase of about 15 nmol O/min/$mg_{protein}$, 50% respiration to an increase of about 45 nmol O/min/$mg_{protein}$ and 100%respiration to an increase of about 85 nmol O/min/$mg_{protein}$. The proton flux estimated for the doubling of the respiration rate was thus increased in the calculations by a factor of 45 divided by 15 to account for 50% respiration, and a factor of 85 divided by 15 to account for 100% respiration. The toxic endpoint 'maximum ATPase activity' was treated the same as maximum uncoupling activity, because maximum ATPase activity seems to correspond to maximum respiration rates at physiologic pH [34]. All gradients and $\Delta\Phi_{H^+}$ used in the respective calculations are stated in Table S2-2.

Literature data

Uncoupling activity data were collected from literature for validation of our predicted uncoupling activities. The collection of EC_w values (see Table S2-2) is by no means exhaustive. Values were selected for the following criteria: (i) It had to be stated by the authors that uncoupling activity was measured, because our model is designed to only predict protonophoric uncoupling activity. Data dominated by other toxic effects such as narcosis or any specific toxicity are therefore not appropriate to test the

performance of the model. If the authors listed additional EC_w values and assumed another toxic mode of action (e.g. Ref. [7]), or if only maximum EC_w were stated, our predictions only served to confirm their hypotheses, but were not used to evaluate the quantitative performance of the model. (ii) The pH at which the experiment was conducted had to be stated. The pH is a critical input parameter to our model, because uncoupling activity is a pH-dependent effect. Uncoupling activity data measured over a broad pH-range was especially searched for. (iii) We narrowed down the data to simple biological systems, such as chromatophores, isolated mitochondria, submitochondrial particles, or intact algae cells. These are all well established in vitro toxicity test methods, yet an extrapolation from in vitro to in vivo is needed. The same is true for our model, as bloodflow, metabolism or similar effects are not considered therein. A comparison to more complex systems was therefore not in the scope of this paper.

The test systems were selected for specific reasons: The dataset measured in chromatophores comprises 35 known protonophoric uncouplers and stands out for its chemical diversity [12]. Although the Kinspec method itself represents no steady-state measurement, it was shown that the EC_w correlate well with EC_w obtained in submitochondrial particles [35], which are very similar to chromatophores with respect to the pH and voltage gradients (positive potential inside, pH lower inside). As long as the uncoupling process is not limited by the back diffusion of the neutral species, Kinspec should be well suited to predict EC_w in submitochondrial particles, and we will treat Kinspec values as such in our calculations. Submitochondrial particles [7,36,37] were selected for their similarity to chromatophores concerning the pH and voltage gradients. Due to these reversed gradients as compared to mitochondria, they are less sensitive to the limiting effects of the neutral permeability. Isolated mitochondria [8,9,13,17,34,38–43] are a very direct test system for measuring uncoupling activity, because in the absence of inhibiting effects the change in respiration rate is a direct indicator for uncoupling activity. Additionally, intact algae cells [10,11,44] were included to show the impact of the ion-trapping effect on uncoupling activity, which leads to a pH-dependence of uncoupling. Concerning pH-dependence, there is a major difference between intact cells, or isolated particles, like

submitochondrial particles, isolated mitochondria, and chromatophores. The change in external pH has a direct influence on uncoupling in isolated systems, because the pH-gradients across the inner membrane change directly. By this, parameters such as fractionation are affected, and thus the concentration equilibrium across the inner membrane changes. Yet, for intact cells, the pH in the cytosol stays relatively stable, and gradients across the inner mitochondrial membrane do not significantly change when the external pH changes. Thus, any pH-dependence does only occur due to de- or increase of the uncoupler concentration across the outer membrane in the cytosol.

Overestimation of uncoupling activity by our model might also result from the fact that with the exception of Ref. [12], literature data did not specifically discern between the total concentration added and the effective freely dissolved concentration in water. The latter is often lower than the former because of sorption to the measurement equipment, partitioning of the compound into the membrane itself or accumulation of the compound inside the cells/particles. These effects can lead to an underestimation of experimental uncoupling activity if the nominal instead of the actual freely dissolved concentration is used. We corrected the EC_w values for the partitioning into the membrane, according to the method provided in Spycher et al. [12]. If no experimental values were available, the membrane/water partition coefficients for both the anionic and neutral species were predicted using COSMOmic [45]. When more detailed information was given, such as the relation between initial and freely dissolved concentration [43], this was used for the correction. If not stated otherwise, corrected values were depicted and used for the calculations.

Results:

We predicted uncoupling activity for 164 compounds, in the four different systems: chromatophores, submitochondrial particles, isolated mitochondria, and intact algae cells. In Figure 2 the experimental effective concentrations EC_w from literature are plotted against the predicted EC_w for all four systems. For the calculations, no specific fit was required, and compound or system specific input parameters

(pK_a, $K_{D,W}$, $P_{A^-_i}$, $P_{A^-_o}$, P_{AH}) were acquired either from experimental values (preferred) or predicted as stated in the Methods section.

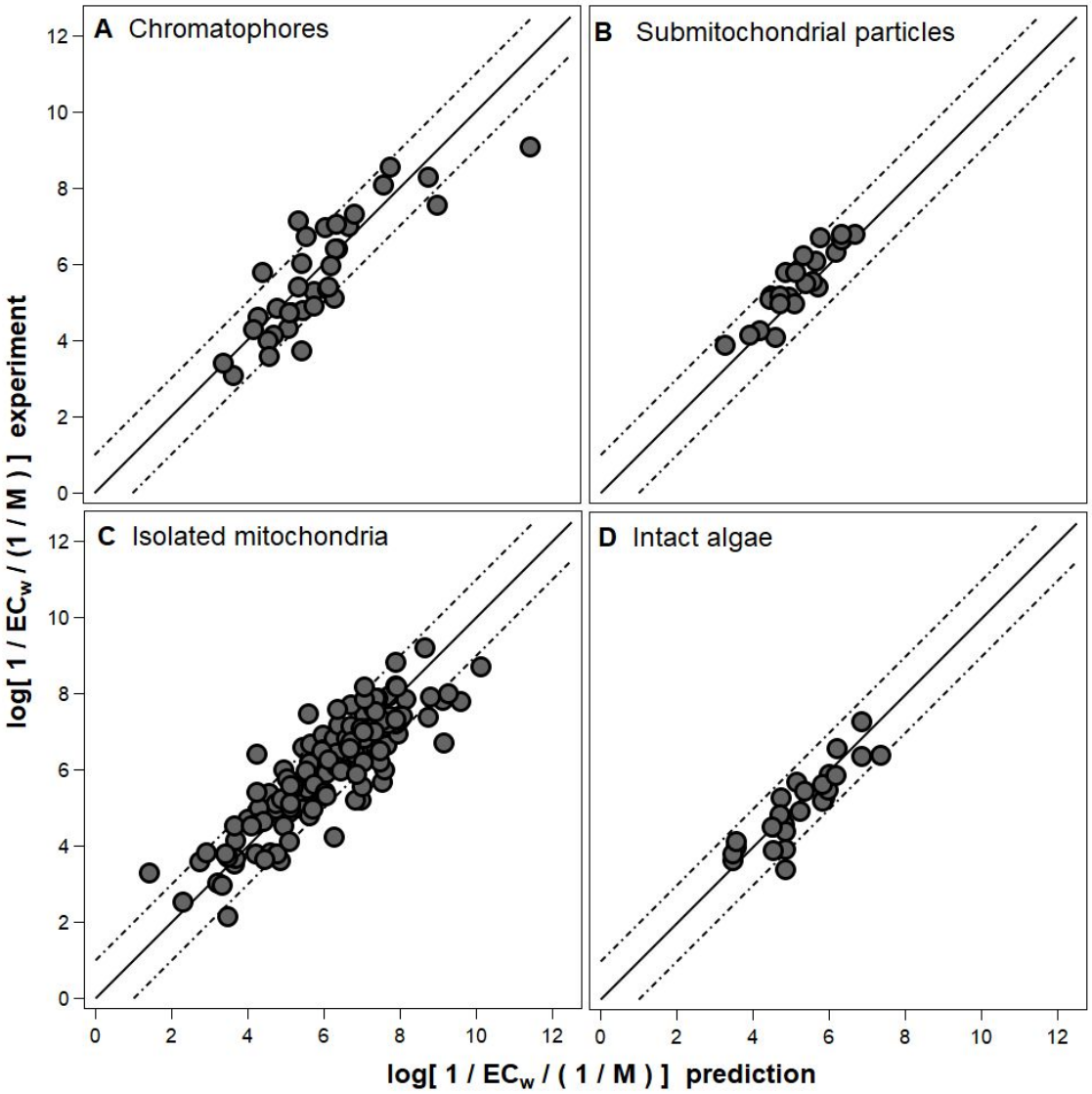

Figure 2 Experimental EC_w from literature in different biological systems plotted against the predictions with the biophysical model (including heterodimer permeation). Experimental data measured for chromatophores (A), submitochondrial particles (B), isolated mitochondria (C) and intact algae cells (D) are listed in Table S2-2 as well as the toxic endpoints. The solid line shows the identity line (1:1); deviations of ±1 log unit are indicated as dashed lines.

Despite the absence of any fit to the specific compound classes or to the toxic endpoints, the root-mean-squared logarithmic error logRMSE of the predictions is below 1 for most datasets (see Table S1-

2), with experimental data spanning about 7 orders of magnitude. The increased logRMSE (0.99) for the prediction of substituted phenols in isolated mitochondria measured by Miyoshi et al. [8,46] could be the consequence of inhibiting effects on respiration. These might lead to an underestimation of the actual experimental uncoupling activity by the chosen toxic endpoint, and thus an overestimation in our model.

In addition to the EC_w value, the output of the model also includes the steady-state fluxes of the respective neutral, anionic, or heterodimeric species across the membrane. This allows us to quantify the influence of heterodimeric permeation, which we will discuss in the following paragraph.

Importance of heterodimer permeation

To implement the permeation of the heterodimer into our model, it was necessary to determine dimerization constants for heterodimers in water. We validated the prediction of heterodimer dimerization constants by comparing the importance of predicted heterodimeric fluxes to that reported in chromatophores in literature (see Section S1-10). The deviations in relative importance of the heterodimer permeation were well below 1.8 orders of magnitude, which would correspond to the expected error range of 10 kJ/mol [20] for the Gibbs free energy of reaction (dimerization) in solution. Yet, predictions for compounds with an intramolecular hydrogen-bond in the neutral monomer seem to be orders of magnitude underestimated. Choosing monomer conformers without this inner bond did improve the prediction, but did not entirely solve the issue. This is not a weakness of the model per se, but of the input parameter, so improvement of the input parameter, be it by experimental value or improved prediction, should increase model performance in the future.

By considering the heterodimeric permeation, the predictions for compounds dominated by monomeric permeation were not affected, while the prediction improved significantly for all compounds dominated by heterodimer permeation. If heterodimer permeation was not considered, uncoupling activity for these compounds was underestimated by up to several orders of magnitude, as can be seen in Figure 3. Here, the monomeric permeation model was used to predict uncoupling

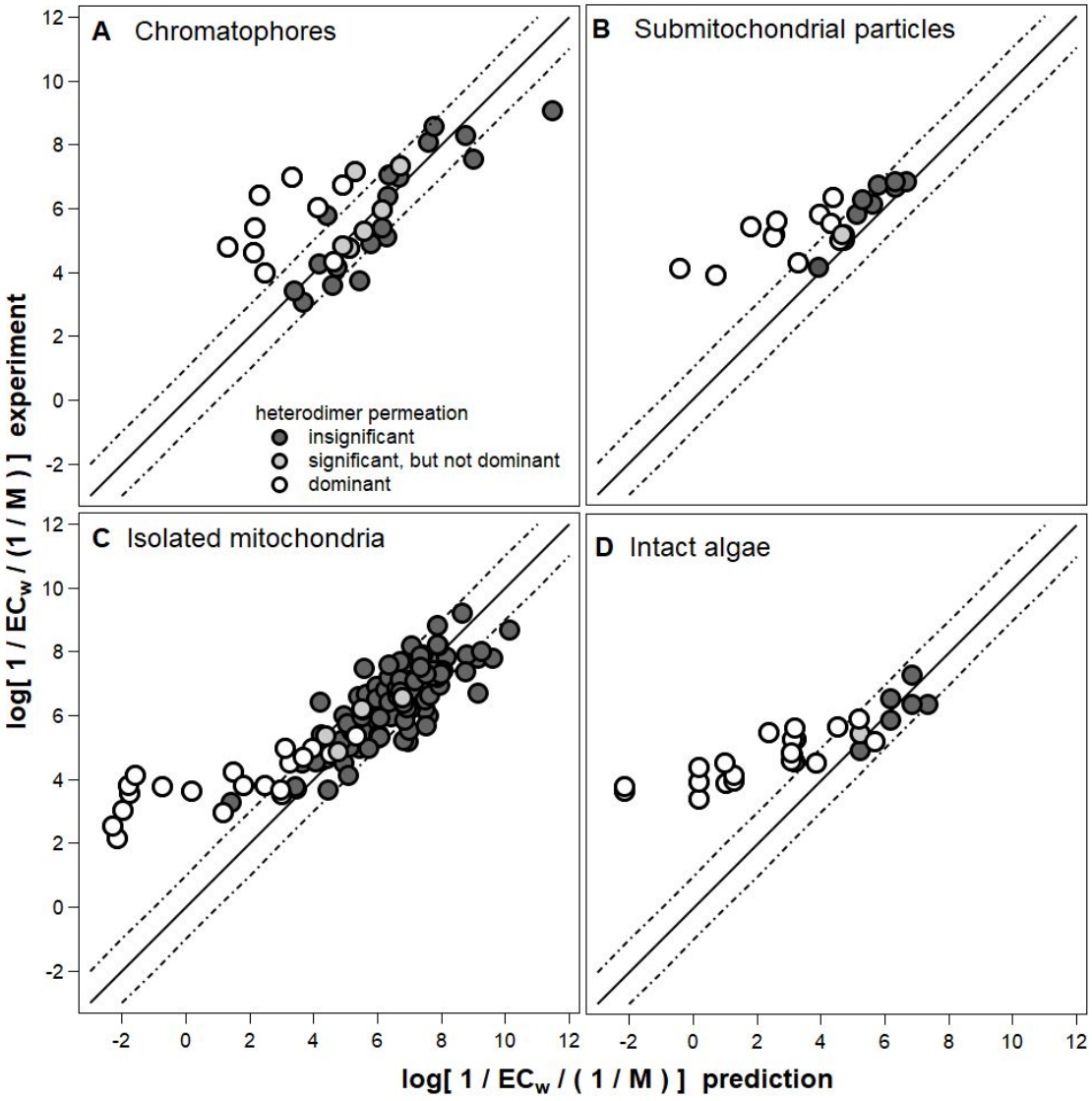

Figure 3 Experimental EC_w from literature in different biological systems plotted against the predictions with the monomeric biophysical model (excluding heterodimer permeation). Experimental data measured for chromatophores (A), submitochondrial particles (B) isolated mitochondria (C) and intact algae cells (D) are listed in Table S2-2, as well as the respective toxic endpoints. The solid line shows the identity line (1:1); deviations of ±1 log unit are indicated as dashed lines. The significance of heterodimer permeation is indicated by the white to dark grey shades of the respective datapoints.

activity. The data points dominated by heterodimer permeation are marked in Figure 3. It is noticeable that the permeation of the heterodimer seems to be dominating especially for those compounds with lower uncoupling activity, where a high compound concentration is needed to reach a critical effect. This promotes a high heterodimer concentration, because the concentration of the heterodimer increases quadratically with the total concentration. The heterodimer concentration is also maximum

at a pH near the pK_a, which explains why the same compound may be dominated by heterodimer permeation in chromatophores, but dominated by monomeric permeation in isolated mitochondria (due to the higher pH), as is the case for 2,4,6-trichlorophenol. For the same reason, namely that the heterodimer concentration is maximum when neutral and anionic fraction are equally high, dominant permeation by the heterodimer and limitation by the neutral permeation seldom coincide. We will discuss in the next paragraph in which cases neutral permeation becomes limiting.

Importance of neutral permeation

Although neutral permeability is usually orders of magnitude higher than ionic permeability of the same molecule, the permeation of the neutral species might become the bottleneck of the uncoupling process if the fraction of neutral species is low. This may be the case for compounds with very low pK_a value, such as 2,4,6-trinitrophenol, or at high pH values. For this reason, uncoupling in chromatophores or submitochondrial particles tends to be less limited by neutral permeation than in mitochondria, because the pH is lower in the inverted systems than in mitochondria (at similar external pH). Using our model with an extremely exaggerated neutral permeability set to 10^6 cm/s, we could calculate the uncoupling activity without limitation by the neutral species. Comparing this value to the actual predicted value allows asserting possible limitations by neutral permeation. Of the compounds analyzed in mitochondria, more than half were limited by the neutral permeation according to our prediction, while for chromatophores only 2,4,6,-trinitrophenol and 3,4-dinitrophenol showed a limitation by neutral permeation. 2,4-dinitrophenol or 2,6-dinitrophenol for example were only limited by the neutral species in mitochondria, but not in chromatophores. This limitation has direct consequences: If neutral permeation dominates the uncoupling process, an increase in pH will decrease the neutral fraction, increase the limiting effect, and therefore decrease uncoupling activity. Observed pH-dependence of uncoupling activities[17,42,47] might thus be explained by the limitation by the neutral permeation. See Figure S1-5 for pH-dependent uncoupling activities due to limitations by the neutral permeation that are also reflected by our model.

Besides low pK_a values, our model also identified very strong uncouplers (-log (EC_w/M) > 6) to be prone to limitation by the neutral permeability. At very high permeabilities, the differences between neutral and ionic permeability may become smaller, because the main resistance of membrane permeation may no more reside in the membrane core, but in the membrane headgroup region. Unfortunately, the prediction of the neutral permeability from the hexadecane/water partition coefficient does not account for this possible limiting effect by the membrane headgroups, and may thus lead to an overestimation of neutral permeability and thus uncoupling activity for very strong uncouplers.

The difference between ionic and neutral permeability is much more pronounced at the outer cell membrane, where ionic permeability is not as high as in the inner mitochondrial membrane. The model was expanded to intact cells by including the permeation balance across this outer cell membrane. The pH-dependent increase or decrease of compound concentration inside the cell due to the ion-trapping effect is well captured by the model, see Figure S1-6. Yet, for the examined compounds in intact algae cells it made no difference if ionic permeation was considered or not.

Despite the influence of heterodimer and neutral permeation, anionic permeability is still the most important input parameter of the model, as will be shown in the next paragraph.

Importance of anionic monomer permeation

To be a potent uncoupler, a compound must have a high anionic membrane permeability. None of the examined uncouplers had a $P_{A^-_i}$ below 10^{-9}cm/s. As long as neither the heterodimer dominates the anionic permeation, nor neutral permeation limits the uncoupling process, the anionic monomer permeation is the key input. One would expect a direct correlation between the uncoupling activity and the anionic membrane permeability of organic chemicals if it is assumed that the limiting process in protonophoric uncoupling lies in the permeability of the anionic species through the hydrocarbon core of the mitochondrial membrane. For these compounds, a simple correlation between uncoupling activity and anionic permeability (times anionic fraction) should already work well. And indeed a

reasonable correlation (r^2=0.84) is found for the dataset measured in chromatophores (see Section S1-13).

Discussion:

The goal of this study was to develop a purely mechanistic model to predict uncoupling activity that explicitly considers potential- or pH- gradients across the membrane. The mechanistic nature of the model provides several advantages: The set of biophysical input parameters (pH, voltage, neutral and anionic permeability, pK_a) can be composed either of experimental or predicted data, as available. For a screening of large datasets which may even be done before any experimental data is available, the model can be used to predict uncoupling activity without any experimental input data, just from the chemical structure of the compound, based on quantum chemical and COSMO-RS calculations for the input parameters. Yet, using experimental input parameters instead of the predicted ones will increase accuracy. If prediction methods or experimental data on single input parameters improve, this will also result in a better performance of the model. We expect the model to have a wide applicability domain because it is not calibrated to any specific dataset. In principle, it should work both for acids and bases. The mechanistic nature of the model also allows drawing direct conclusions on the impact of single input factors. We were thus able to explain the pH-dependent uncoupling activity of 2,4-DNP and 2,6-DNP, for which the uncoupling activity is not limited by the permeation of the anionic species but by that of the neutral species. The pH-dependence is therefore explainable in agreement with Mitchell's chemiosmotic theory, contrary to the statement of Nath [17].

Comparison to QSARs

In a direct comparison of our model's logRMSE to the standard deviation in typical QSAR studies, our deviations are higher. For example, Miyoshi et al. [8] (QSAR: 0.27 ;our model: 0.76;N=22 (datasubset 13, see Table S2-2);regression coefficients: 5), Argese et al. [7] (QSAR: 0.15 ;our model: 0.63;N=7 (datasubset 14);regression coefficients: 2), Terada et al. [9] (QSAR: 0.37 ;our model: 0.61;N=25 (dataset 9);regression

coefficients: 3) all showed lower standard deviations. This is to be expected, because these authors used regressions, often with multiple regression coefficients, and did not discern between training and testing data. Their fits are specific to the examined compound class and experimental setup, and often vary widely if compared to each other. In contrast, our model is completely mechanistic with a wide applicability domain.

A more sophisticated QSAR was presented by Spycher et al. [12], who sought to extend the applicability domain of their model across several compound classes using a diverse dataset. To validate their model, they divided their dataset in test and training data, or did a cross validation to assess the predictive power for the training set. Using our model to predict the values in the training set (N=17; datasubset 15) or test set (N=8; datasubset 16), we get logRMSE values (test: 0.79; training: 0.57) comparable to their standard deviations for their best regression depending on experimental liposome /water partition coefficients (test: 0.61; training: 0.56) or depending on predicted liposome/water partition coefficients (test: 0.86; training: 0.99). But in contrast to our model, it will overestimate uncoupling activity for those compounds limited by the neutral permeability, and the prediction is limited to pH7 in chromatophores, because neither the possible limiting effect of the permeation of the neutral species, nor pH- and electrical gradients across the membrane are considered in their model.

Current reliability of input parameters

The performance of the model itself strongly depends on the availability of reliable experimental or predicted input parameters. While prediction of the pK_a is quite reliable (logRMSE for compounds examined here: 0.86), prediction of the neutral permeability seems to be less reliable. Overestimations of the charge separation in DFT (density functional theory) calculations for compounds containing $-NO_2$ and $-C\equiv N$ groups [48] may lead to an underestimation of the partition coefficient calculated with COSMOtherm and thus of the neutral permeability. It is also important to consider different tautomers, because their predicted partition coefficients can differ by several orders of magnitude (up to 4 orders of magnitude deviations, see Table S2-1). The neutral permeability may also be overestimated, as is

the case for 3-tert-butyl-5-chloro-N-(2-chloro-4-nitrophenyl)-2-hydroxybenzamide (S-13; 3 orders of magnitude). It was already speculated in the past that for very hydrophobic compounds, the main resistance for membrane permeation might no longer reside in the membrane core, but in the membrane headgroup region [49]. Also, a linear relationship with the hexadecane/water partition coefficient has only been shown up to about P=10 cm/s [30]. This would lead to an overestimation of membrane permeability if only the membrane core is considered in the calculation, as is the case for the correlation based on the chlorodecane/water partition coefficient. A method to predict permeabilities that considers the anisotropy along the membrane normal might thus in the future improve the performance of the model. COSMOperm [15] might be a promising prediction method in this respect. Testing different prediction methods was not in the scope of this manuscript, as it focused on the model itself, but a performance optimization based on an improved prediction of the input parameters is a goal for the near future.

Also for charged compounds, the linear relationship between the ionic permeability and the hexadecane/water partition coefficient has only been shown up to about P = 10 cm/s [14]. Thus, also there it seems possible that the headgroup regions of the membrane might represent the main resistance for ionic permeation for very hydrophobic compounds (see Figure S1-7), an assumption that would explain the large overestimation in uncoupling activity for the compound fluazinam in chromatophores.

The prediction of dimerization constants gave mostly reliable results, with the exceptions of compounds containing nitro-groups that formed intramolecular hydrogen bonds in the neutral monomer. In their case, the dimerization constant was underestimated by several orders of magnitude. This possible error has to be kept in mind when predicting dimerization constants and should be addressed in the future. Yet, it did not have a significant effect on the prediction of uncoupling toxicity itself, as for none of the concerned compounds tested here heterodimer permeation strongly dominated.

Conclusion:

The validation datasets were mostly composed of rather similar structures, such as phenols, trifluoromethylbenzimidazoles, hydrazones and salicylanilides, as these are typical protonophoric uncouplers. Nevertheless, our mechanistic model should allow screening of diverse datasets for possible uncoupling activity. The ab initio approach to predict our input parameters (COSMOtherm/Turbomole) should even allow identifying new uncouplers that would not be triggered by conventional structure alert approaches (such as Ref. [50]).

One of the key features of our model, the formation and diffusion of heterodimers through the membrane, has already been observed by a quadratic dependence of electrical conductivity on uncoupler concentration in black lipid membrane systems (e.g. [31,51,52]) and in chromatophores [18]. While it has been speculated about heterodimer permeation in submitochondrial particles [53], we could not find evidence in literature for heterodimer permeation in mitochondria. Nevertheless, the better match of our calculations to the experimental EC_w if heterodimer permeation is considered suggests that this phenomenon may also be relevant in mitochondria.

The model on its own only predicts the uncoupling activity of a chemical. Here we have assumed that this uncoupling activity generally leads to a toxic effect when the respiration rate is doubled. This general threshold could be replaced by a more specific threshold for specific toxic endpoints. This would lead to better results in the specific case, but limit its application to that domain. Also, the user will have to check whether the predicted uncoupling activity lies within the range of compound solubility, or if other toxic effects such as baseline toxicity or any specific toxicity will dominate the toxic effect. This could be an advantage: In combination with a model for baseline toxicity, the model may be used to detect specific toxic effects by comparing predicted to overall experimental toxicity.

We expect the performance of the model to improve with the accuracy of the predicted input parameters. Recent developments in predicting cationic membrane permeability [15] might in the future allow to extend the model to basic uncouplers. While uncoupling due to weak bases is rare and expected to be rather mild, and thus most weak base uncouplers should have negligible toxic effects, this makes them interesting candidates for therapeutic use [54].

Funding Information.

The authors Andrea Ebert and Kai Uwe Goss declare no competing financial interest.

Acknowledgements.

We would like to thank the German athletes of the international chemistry olympiad 2019 who proposed designs for our TOC graphic during their visit to our institution. Special thanks go to Richard Eckhardt and Maximilian Mittl, whose design finally inspired our TOC graphic. The scientific results have (in part) been computed at the High-Performance Computing (HPC) Cluster EVE, a joint effort of both the Helmholtz Centre for Environmental Research - UFZ (http://www.ufz.de/) and the German Centre for Integrative Biodiversity Research (iDiv) Halle-Jena-Leipzig (http://www.idiv-biodiversity.de/). We would like to thank the administration and support staff of EVE who keep the system running and support us with our scientific computing needs: Thomas Schnicke, Ben Langenberg, Guido Schramm and Tom Strempel from the UFZ, and Christian Krause from iDiv.

SI statement.

List of abbreviations, detailed model derivations, comparison between experimental and predicted pKa, typical pH- and voltage gradients, estimation of H+ flux, logRMSE of different datasets, validation of hetero-dimerization constant, plots of pH-dependent EC_w, correlation between EC_w and anionic permeability, anionic resistance profile of fluazinam (SI-1.pdf)

Table S2-1 (list of input parameters) and Table S2-2 (list of EC_w) (SI-2.xlsx)

IgorPro script for numerical calculations (SI-3.txt)

References.

(1) Mitchell, P. Coupling of Phosphorylation to Electron and Hydrogen Transfer by a Chemi-Osmotic Type of Mechanism. *Nature* **1961**, *191* (4784), 144–148. https://doi.org/10.1038/191144a0.

(2) Loomis, W. F.; Lipmann, F. Reversible Inhibition of the Coupling between Phosphorylation and Oxidation. *J .Biol. Chem.* **1948**, No. 172, 807–808.

(3) Terada, H. Uncouplers of Oxidative Phosphorylation. *Environ. Health Perspect.* **1990**, *87*, 213–218. https://doi.org/10.1289/ehp.9087213.

(4) Pierelli, G.; Stanzione, R.; Forte, M.; Migliarino, S.; Perelli, M.; Volpe, M.; Rubattu, S. Uncoupling Protein 2: A Key Player and a Potential Therapeutic Target in Vascular Diseases. *Oxid. Med. Cell. Longev.* **2017**, *2017*. https://doi.org/10.1155/2017/7348372.

(5) Skulachev, V. P. Energy Transformations in the Respiratory Chain. *Curr. Top. Bioenerg.* **1971**, *4* (C), 127–190. https://doi.org/10.1016/B978-0-12-152504-0.50010-1.

(6) Cajina-Quezada, M.; Wayne Schultz, T. Structure-Toxicity Relationships for Selected Weak Acid Respiratory Uncouplers. *Aquat. Toxicol.* **1990**, *17* (3), 239–252. https://doi.org/10.1016/0166-445X(90)90066-X.

(7) Argese, E.; Bettiol, C.; Marchetto, D.; De Vettori, S.; Zambon, A.; Miana, P.; Ghetti, P. F. Study on the Toxicity of Phenolic and Phenoxy Herbicides Using the Submitochondrial Particle Assay. *Toxicol. Vitr.* **2005**, *19* (8), 1035–1043. https://doi.org/10.1016/j.tiv.2005.05.004.

(8) Miyoshi H Tsujisjita H, T. N.; T, F. Quantitative Analysis of Uncoupling Activity of Substituted Phenols... *Biochim. Biophys. Acta* **1990**, *1016*, 99–106. https://doi.org/10.1016/0005-2728(90)90011-R.

(9) Terada, H.; Goto, S.; Yamamoto, K.; Takeuchi, I.; Hamada, Y.; Miyake, K. Structural Requirements of Salicylanilides for Uncoupling Activity in Mitochondria: Quantitative Analysis of Structure-Uncoupling Relationships. *BBA - Bioenerg.* **1988**, *936* (3), 504–512. https://doi.org/10.1016/0005-2728(88)90027-8.

(10) Shigeoka, T.; Sato, Y.; Takeda, Y.; Yoshida, K.; Yamauchi, F. Acute Toxicity of Chlorophenols to Green Algae, Selenastrum Capricornutum and Chlorella Vulgaris, and Quantitative Structure-activity Relationships. *Environ. Toxicol. Chem.* **1988**, *7* (10), 847–854. https://doi.org/10.1002/etc.5620071007.

(11) Chen, C. Y.; Lin, J. H. Toxicity of Chlorophenols to Pseudokirchneriella Subcapitata under Air-Tight Test Environment. *Chemosphere* **2006**, *62* (4), 503–509. https://doi.org/10.1016/j.chemosphere.2005.06.060.

(12) Spycher, S.; Smejtek, P.; Netzeva, T. I.; Escher, B. I. Toward a Class-Independent Quantitative Structure - Activity Relationship Model for Uncouplers of Oxidative Phosphorylation. *Chem. Res. Toxicol.* **2008**, *21* (4), 911–927. https://doi.org/10.1021/tx700391f.

(13) Dilger, J.; McLaughlin, S. Proton Transport through Membranes Induced by Weak Acids: A Study of Two Substituted Benzimidazoles. *J. Membr. Biol.* **1979**, *46* (4), 359–384. https://doi.org/10.1007/BF01868755.

(14) Ebert, A.; Hannesschlaeger, C.; Goss, K.-U.; Pohl, P. Passive Permeability of Planar Lipid Bilayers to Organic Anions. *Biophysj* **2018**, *115* (10), 1931–1941. https://doi.org/10.1016/j.bpj.2018.09.025.

(15) Schwöbel, J. A. H.; Ebert, A.; Bittermann, K.; Huniar, U.; Goss, K.-U.; Klamt, A. COSMO Perm: Mechanistic Prediction of Passive Membrane Permeability for Neutral Compounds and Ions and Its PH Dependence. *J. Phys. Chem. B* **2020**. https://doi.org/10.1021/acs.jpcb.9b11728.

(16) Baumer, A.; Bittermann, K.; Klüver, N.; Escher, B. I. Baseline Toxicity and Ion-Trapping Models to Describe the PH-Dependence of Bacterial Toxicity of Pharmaceuticals. *Environ. Sci. Process. Impacts* **2017**, *19* (7), 901–916. https://doi.org/10.1039/C7EM00099E.

(17) Nath, S. Molecular Mechanistic Insights into Uncoupling of Ion Transport from ATP Synthesis. *Biophys. Chem.* **2018**, *242* (July), 15–21. https://doi.org/10.1016/j.bpc.2018.08.006.

(18) Escher, B. I.; Snozzi, M.; Schwarzenbach, R. P. Uptake, Speciation, and Uncoupling Activity of Substituted Phenols in Energy Transducing Membranes. *Environ. Sci. Technol.* **1996**, *30* (10), 3071–3079. https://doi.org/10.1021/es960153f.

(19) Finkelstein, A. Weak-Acid Uncouplers of Oxidative Phosphorylation. Mechanism of Action on Thin Lipid Membranes. *BBA - Bioenerg.* **1970**, *205* (1), 1–6. https://doi.org/10.1016/0005-2728(70)90055-1.

(20) Hellweg, A.; Eckert, F. Brick by Brick Computation of the Gibbs Free Energy of Reaction in Solution Using Quantum Chemistry and COSMO-RS. *AIChE J.* **2017**, *63* (9), 3944–3954. https://doi.org/10.1002/aic.15716.

(21) Sachsenhauser, T.; Rehfeldt, S.; Klamt, A.; Eckert, F.; Klein, H. Consideration of Dimerization for Property Prediction with COSMO-RS-DARE. *Fluid Phase Equilib.* **2014**, *382*, 89–99. https://doi.org/10.1016/j.fluid.2014.08.030.

(22) Eckert, F.; Klamt, A. Fast Solvent Screening via Quantum Chemistry: COSMO-RS Approach. *AIChE J.* **2002**, *48* (2), 369–385. https://doi.org/10.1002/aic.690480220.

(23) Gutknecht, J. Salicylates and Proton Transport through Lipid Bilayer Membranes: A Model for Salicylate-Induced Uncoupling and Swelling in Mitochondria. *J. Membr. Biol.* **1990**, *115* (3), 253–260. https://doi.org/10.1007/BF01868640.

(24) Dilger, J.; Mclaughlin, S.; McIntosh, T. J.; Simon, S. A. The Dielectric Constant of Phospholipid Bilayers and the Permeability of Membranes to Ions. *Science* **1979**, *206* (4423), 1196–1198. https://doi.org/10.1126/science.228394.

(25) COSMOtherm, Release 18. COSMOlogic GmbH & Co. KG; http://www.cosmologic.de: Leverkusen, Germany, 2018.

(26) TURBOMOLE V7.3. University of Karlsruhe and Forschungszentrum Karlsruhe GmbH, 1989-2007, TURBOMOLE GmbH, since 2007; available from http://www.turbomole.com: Karlsruhe, Germany, 2018.

(27) COSMOconf 4.1. COSMOlogic GmbH & Co. KG; http://www.cosmologic.de: Leverkusen, Germany, 2016.

(28) Hannesschlaeger, C.; Horner, A.; Pohl, P. Intrinsic Membrane Permeability to Small Molecules. *Chem. Rev.* **2019**, *119* (9), 5922–5953. https://doi.org/10.1021/acs.chemrev.8b00560.

(29) Walter, A.; Gutknecht, J. Permeability of Small Nonelectrolytes through Lipid Bilayer Membranes. *J. Membr. Biol.* **1986**, *90* (3), 207–217. https://doi.org/10.1007/BF01870127.

(30) Bittermann, K.; Goss, K.-U. Predicting Apparent Passive Permeability of Caco-2 and MDCK Cell-Monolayers: A Mechanistic Model. *PLoS One* **2017**, *12* (12), 1–20. https://doi.org/10.1371/journal.pone.0190319.

(31) Gutknecht, J. Aspirin, Acetaminophen and Proton Transport through Phospholipid Bilayers and Mitochondrial Membranes. *Mol. Cell. Biochem.* **1992**, *114* (1–2), 3–8. https://doi.org/10.1007/BF00240290.

(32) JChem for Office 20.2.0.589. ChemAxon (http://www.chemaxon.com) 2020.

(33) Nicholls, D. G.; Ferguson, S. Bioenergetics: Fourth Edition. In *Bioenergetics: Fourth Edition*; Academic Press, 2013; pp 1–419. https://doi.org/10.1016/C2010-0-64902-9.

(34) Parker, V. Uncouplers of Rat-Liver Mitochondrial Oxidative Phosphorylation. *Biochem. J.* **1965**,

97 (3), 658–662. https://doi.org/10.1042/bj0970658.

(35) Escher, B. I.; Snozzi, M.; Häberli, K.; Schwarzenbach, R. P. A New Method for Simultaneous Quantification of Uncoupling and Inhibitory Activity of Organic Pollutants in Energy-Transducing Membranes. *Environ. Toxicol. Chem.* **1997**, *16* (3), 405–414. https://doi.org/10.1897/1551-5028(1997)016<0405:ANMFSQ>2.3.CO;2.

(36) Argese, E.; Bettiol, C.; Ghelli, A.; Todeschini, R.; Miana, P. Submitochondrial Particles as Toxicity Biosensors of Chlorophenols. *Environmental Toxicology and Chemistry*. 1995, pp 363–368. https://doi.org/10.1002/etc.5620140302.

(37) Hanstein, W. Trinitrophenol: A Membrane-Impermeable Uncoupler of Oxidative Phosphorylation. *Proc. Natl. Acad. Sci.* **1974**, *71* (2), 288–292. https://doi.org/10.1073/pnas.71.2.288.

(38) McCracken, R. O.; Carr, A. W.; Stillwell, W. H.; Lipkowitz, K. B.; Boisvenue, R.; O'doherty, G. O. P.; Wickiser, D. I. Trifluoromethanesulfonamide Anthelmintics Protonophoric Uncouplers of Oxidative Phosphorylation. *Biochem. Pharmacol.* **1993**, *45* (9), 1873–1880. https://doi.org/10.1016/0006-2952(93)90446-4.

(39) Miyoshi, H.; Fujita, T. Quantitative Analyses of Uncoupling Activity of SF6847 (2,6-Di-t-Butyl-4-(2,2-Dicyanovinyl)Phenol) and Its Analogs with Spinach Chloroplasts. *BBA - Bioenerg.* **1987**, *894* (2), 339–345. https://doi.org/10.1016/0005-2728(87)90204-0.

(40) McDougall, P.; Markham, A.; Cameron, I.; Sweetman, A. J. Action of the Nonsteroidal Anti-Inflammatory Agent, Flufenamic Acid, on Calcium Movements in Isolated Mitochondria. *Biochem. Pharmacol.* **1988**, *37* (7), 1327–1330. https://doi.org/10.1016/0006-2952(88)90790-3.

(41) Jones, B. T. G.; Watson, W. A. Properties of Substituted 2-Trifluoromethylbenzimidazoles Uncouplers of Oxidative Phosphorylation. **1967**, 564–573. https://doi.org/10.1042/bj1020564.

(42) Hemker, H. C. Inhibition of Adenosine Triphosphatase and Respiration of Rat-Liver Mitochondria by Dinitrophenols. *BBA - Enzymol. Subj.* **1964**, *81* (1), 1–8. https://doi.org/10.1016/0926-6569(64)90329-3.

(43) Baláž, Š.; Šturdík, E.; Ďurčová, E.; Antalík, M.; Sulo, P. Quantitative Structure-Activity Relationship of Carbonylcyanide Phenylhydrazones as Uncouplers of Mitochondrial Oxidative Phosphorylation. *BBA - Bioenerg.* **1986**, *851* (1), 93–98. https://doi.org/10.1016/0005-2728(86)90252-5.

(44) Walter, H.-A. *Kombinationswirkungen von Umweltchemikalien*; doctoral dissertation; ISBN-10: 3936231869., 2002.

(45) Bittermann, K.; Spycher, S.; Endo, S.; Pohler, L.; Huniar, U.; Goss, K.-U.; Klamt, A. Prediction of Phospholipid-Water Partition Coefficients of Ionic Organic Chemicals Using the Mechanistic Model COSMOmic. *J. Phys. Chem. B* **2014**, *118* (51), 14833–14842. https://doi.org/10.1021/jp509348a.

(46) Miyoshi, H.; Fujita, T. Quantitative Analyses of the Uncoupling Activity of Substituted Phenols with Mitochondria from Flight Muscles of House Flies. *BBA - Bioenerg.* **1988**, *935* (3), 312–321. https://doi.org/10.1016/0005-2728(88)90226-5.

(47) Wilson, D. F.; Ting, H. P.; Koppelman, M. S. Mechanism of Action of Uncouplers of Oxidative Phosphorylation. *Biochemistry* **1971**, *10* (15), 2897–2902. https://doi.org/10.1021/bi00791a016.

(48) Reinisch, J.; Diedenhofen, M.; Wilcken, R.; Udvarhelyi, A.; Glöß, A. Benchmarking Different

QM Levels for Usage with COSMO-RS. *J. Chem. Inf. Model.* **2019**. https://doi.org/10.1021/acs.jcim.9b00659.

(49) Diamond, J. M.; Katz, Y. Interpretation of Nonelectrolyte Partition Coefficients between Dimyristoyl Lecithin and Water. *J. Membr. Biol.* **1974**, *17* (1), 121–154. https://doi.org/10.1007/BF01870176.

(50) Enoch, S. J.; Schultz, T. W.; Popova, I. G.; Vasilev, K. G.; Mekenyan, O. G. Development of a Decision Tree for Mitochondrial Dysfunction: Uncoupling of Oxidative Phosphorylation. *Chem. Res. Toxicol.* **2018**, *31* (8), 814–820. https://doi.org/10.1021/acs.chemrestox.8b00132.

(51) Foster, M.; McLaughlin, S. Complexes between Uncouplers of Oxidative Phosphorylation. *J. Membr. Biol.* **1974**, *17* (1), 155–180. https://doi.org/10.1007/BF01870177.

(52) Smejtek, P.; Hsu, K.; Perman, W. H. Electrical Conductivity in Lipid Bilayer Membranes Induced by Pentachlorophenol. *Biophys. J.* **1976**, *16* (4), 319–336. https://doi.org/10.1016/S0006-3495(76)85691-3.

(53) Argese, E.; Bettiol, C.; Giurin, G.; Miana, P. Quantitative Structure-Activity Relationships for the Toxicity of Chlorophenols to Mammalian Submitochondrial Particles. *Chemosphere* **1999**, *38* (10), 2281–2292. https://doi.org/10.1016/S0045-6535(98)00446-9.

(54) Antonenko, Y. N.; Avetisyan, A. V.; Cherepanov, D. A.; Knorre, D. A.; Korshunova, G. A.; Markova, O. V.; Ojovan, S. M.; Perevoshchikova, I. V.; Pustovidko, A. V.; Rokitskaya, T. I.; et al. Derivatives of Rhodamine 19 as Mild Mitochondria-Targeted Cationic Uncouplers. *J. Biol. Chem.* **2011**, *286* (20), 17831–17840. https://doi.org/10.1074/jbc.M110.212837.